system helps determine the T or physical state of the planetary cores. The eutectic T determined in this study is 860°C at 18 GPa, which is about 500°C less than that extrapolated from (2). The extrapolation to higher P based on (2) could result in the overestimation of core T. In fact, such extrapolation should not be exercised in the Fe-FeS system because of the formation of the intermediate compound and changes in physical properties of end-member FeS (10) at high P and T. Theoretical calculations also showed that other Fe-S compounds such as Fe_3S could form at higher P (11), and melting relations in the Fe-FeS system at the core P of the Earth (135 to 360 GPa) may be different from what we observed at relatively low P. In addition, the presence of Ni in the system could further complicate the phase relations.

Iron sulfides are found in many classes of meteorites. If Fe_3S_2 were indeed found in a meteorite, it would indicate the minimum size of the parent body and the maximum T of the core. The Fe_3S_2 compound could only be found in meteorites that come from parent bodies with a center $P > 14$ GPa and T less than the eutectic temperature (which is ~900°C, depending on the pressure).

REFERENCES AND NOTES

1. F. Birch, *J. Geophys. Res.* **69**, 4377 (1964); B. Mason, *Nature* **211**, 616 (1966); V. R. Murthy and H. T. Hall, *Phys. Earth Planet. Inter.* **2**, 276 (1970); J. M. Brown, T. J. Ahrens, D. L. Shampine, *J. Geophys. Res.* **89**, 6041 (1984); H. Wänke and G. Dreibus, *Philos. Trans. R. Soc. London Ser. A* **235**, 545 (1988); Q. Williams and R. Jeanloz, *J. Geophys. Res.* **95**, 19299 (1990); R. Boehler, *Earth Planet. Sci. Lett.* **111**, 217 (1992).
2. T. M. Usselman, *Am. J. Sci.* **275**, 278 (1975).
3. R. Brett and P. M. Bell, *Earth Planet. Sci. Lett.* **6**, 479 (1969).
4. B. Ryzhenko and G. C. Kennedy, *Am. J. Sci.* **273**, 803 (1973).
5. M. Hansen and K. Anderko, *Constitution of Binary Alloys* (McGraw-Hill, New York, 1958), p. 704.
6. Experimental techniques were described by C. M. Bertka and Y. Fei (*J. Geophys. Res.*, in press). The starting materials, Fe-FeS mixtures, were synthesized in evacuated, sealed silica glass tubes at 800°C. The starting materials were then loaded in a MgO-platinum or a MgO-rhenium double-capsule. Experiments below 3 GPa were conducted in a piston-cylinder apparatus. At higher pressures, melting experiments were carried out in a multi-anvil apparatus. The apparatus has been calibrated up to a pressure of 25 GPa for a 10-mm-edged octahedron and 3-mm TEL (truncation edge length) assembly at both room temperature and 1200°C. The 3-mm assembly consisted of a rhenium heater with a lanthanum chromite sleeve serving as a thermal insulator. Temperatures were measured with a W26%Re–W5%Re thermocouple whose hot junction was in direct contact with the sample container. The eutectic temperature was bracketed by a series of quenched experiments carried out at different temperatures.
7. Quantitative chemical analyses were obtained with a JEOL JXA-8900 electron microprobe, using pyrite FeS_2 as a standard. The composition of the samples synthesized at 14 GPa is very close to stoichiometric Fe_3S_2 (27.7% S). The compound may be of nonstoichiometric nature, because the samples synthesized at 18 GPa have a lower sulfur content (27.1 ± 0.2% S) than does Fe_3S_2 stoichiometric composition.
8. Powder x-ray diffraction data were collected at beam line X7A of the National Synchrotron Light Source of Brookhaven National Laboratory, using the high-resolution mode with a Si(111) channel-cut monochromator and a Ge(110) analyzer crystal at 0.79826(2) Å. See D. E. Cox, B. H. Toby, M. M. Eddy [*Aust. J. Phys.* **41**, 117 (1988)] for details of the instrument. The wavelength and diffractometer zero were calibrated with Si powder. Program GSAS [A. C. Larson and R. B. Von Dreele, *Report LA-UR 86-748* (Los Alamos National Laboratory, Los Alamos, NM, 1986)] was used for all profile fitting. A modified version of TREOR90 [P.-E. Werner, L. Eriksson, M. J. Westdahl, *J. Appl. Crystallogr.* **18**, 367 (1985)] was used to determine the unit-cell parameters for the unknown phases. For the method of intensity extraction, see A. Le Bail, H. Duray, J. L. Fourquet [*Mater. Res. Bull.* **23**, 447 (1988)]. The intensity values do not imply any knowledge of the crystal structures of these phases.
9. G. Kullerud and R. A. Yund, *J. Petrol.* **3**, 126 (1962); M. E. Fleet, *Am. Mineral.* **62**, 341 (1977); J. B. Parise, *Acta Crystallogr. B* **36**, 1179 (1980).
10. Y. Fei, C. T. Prewitt, H.-k. Mao, C. M. Bertka, *Science* **268**, 1892 (1995).
11. D. M. Sherman, *Earth Planet. Sci. Lett.* **132**, 87 (1995).

12. We thank A. Campbell for carrying out some of the experiments at $P < 12$ GPa. Supported by the NASA Planetary Materials and Geochemistry Program (NAGW-3942), the NSF Center for High Pressure Research, and the Carnegie Institution of Washington.

1 November 1996; accepted 29 January 1997

Melting of $(Mg,Fe)_2SiO_4$ at the Core-Mantle Boundary of the Earth

Kathleen G. Holland and Thomas J. Ahrens

The lower mantle of the Earth is believed to be largely composed of (Mg,Fe)O (magnesiowüstite) and $(Mg,Fe)SiO_3$ (perovskite). Radiative temperatures of single-crystal olivine $[(Mg_{0.9},Fe_{0.1})_2SiO_4]$ decreased abruptly from 7040 ± 315 to 4300 ± 270 kelvin upon shock compression above 80 gigapascals. The data indicate that an upper bound to the solidus of the magnesiowüstite and perovskite assemblage at 4300 ± 270 kelvin is 130 ± 3 gigapascals. These conditions correspond to those for partial melting at the base of the mantle, as has been suggested occurs within the ultralow-velocity zone beneath the central Pacific.

The major minerals of Earth's lower mantle are thought to be $(Mg_{0.94},Fe_{0.06})SiO_3$ perovskite and $(Mg_{0.84},Fe_{0.16})O$ magnesiowüstite (1). Thus, the melting behavior of this assemblage is important for determining the temperature of the mantle and the origin of the seismically imaged structures at the core-mantle boundary (CMB). Recent studies of the solidi of this mantle assemblage are disparate: The melting temperature of pure $MgSiO_3$ perovskite (Pv) at the CMB has been estimated at 7000 to 8500 K (2) and 4500 ± 350 K (3). Measurements of the melting of MgO [periclase (Per)] at pressures up to 31.5 GPa (4000 ± 200 K) (4) imply, when extrapolated to 133 GPa, that it melts at 5100 ± 750 K. Phase equilibrium experiments (5) demonstrate that at lower mantle pressures, the stable high-pressure phase (hpp) assemblage for Mg_2SiO_4 [forsterite (Fo)] is MgO (Per) + $MgSiO_3$ (Pv); thus, Fo can be used as a representative starting material in shock experiments. Syono and co-workers' (6) shock-recovery experiments on Fo indicate that MgO (Per) + $MgSiO_3$ (glass that is inferred to have been Pv at high pressure and temperature) is actually recovered from samples that were at high pressure for the short (10^{-7} s) time scale of a shock-wave experiment (6). In previous shock experiments using olivine crystals, Brown *et al.* (7) inferred the onset of melting of the assemblage Per + Pv above ~140 GPa on the basis of a sharp decrease in longitudinal elastic wave velocity. Brown *et al.* (7) also suggested that the previous shock temperatures measured in Fo in the range of 160 to 180 GPa (8) are representative of the liquid regime of the Fo Hugoniot. Because Fo shocked below 160 GPa has a low Planck emissivity, temperatures in the pressure range where the Hugoniot curve crosses the solidus (~90 to 133 GPa) were not measurable. Here, we determine the onset of melting at lower pressures using higher emissivity olivine samples and a more sensitive detector system (9). We used samples of San Carlos and Burma peridot $[(Mg_{0.9},Fe_{0.1})_2SiO_4$ (10)] for shock-temperature experiments because they are green rather than transparent. Their ambient-condition emissivities are ~0.7 and ~1.0 at 560 and 900 nm. Moreover, their solidi are within 110°C of the melting point of Fo at 1 bar (5). Using 5 mm by 5 mm by 2 mm samples, we conducted measurements from 94 to 192 GPa (Table 1) (11). As the shock wave propagated through the sample (12), the com-

Lindhurst Laboratory of Experimental Geophysics, Seismological Laboratory, California Institute of Technology, Pasadena, CA 91125, USA.

pressed region emitted thermal radiation, which then propagated through the absorbing unshocked sample (Fig. 1). As the shock front propagated through the sample, the radiation from the shock front was attenuated by successively less unshocked sample; thus, radiance increased with time (*13*) (Fig. 2A). For each experiment, signals ~300 ns long were recorded by photodiodes in six wavelength bands from 450 to 900 nm. Data corrected for mineral emissivity and system response (*14*, *15*) were fitted to a Planck function to obtain emissivity and temperature (Fig. 2, B through D). Shock temperatures were nearly constant (Fig. 2C) during propagation through the sample, whereas the irradiance (Fig. 2A) varied with emissivity (Fig. 2C).

We determined shock temperatures of peridot in eight experiments (Table 1 and Fig. 3). Between 127 and 133 GPa, we measured a change in temperature from 7041 ± 315 to 4292 ± 270 K. The data for peridot and earlier data (*8*) for the shock-induced melt of the high-pressure assemblage of Fo appear to agree. We infer that the difference in shock temperature observed between the 127- and 133-GPa experiments results from our sampling the lower pressure, superheated (solid) hpp assemblage and the onset of melting with increasing shock pressure. This behavior is analogous to that in SiO_2 and alkali halides (*16*, *17*). Because a material will not melt if its temperature does not exceed the solidus at the relevant pressure, the observed shock temperature of 4300 ± 270 K represents an upper bound to the solidus at 130 ± 3 GPa. Our estimate is consistent with a solidus attained for $(Mg_{0.9},Fe_{0.1})_2SiO_4$ at lower pressure reported by Presnall and Walter (*18*). There is the possibility that the onset of melting could be overdriven by kinetic effects (*17*), so our estimated solidus is an upper bound.

In analogy to low-pressure data, we suggest that in the MgO-$MgSiO_3$ system, the high-pressure lower mantle assemblage can undergo eutectic melting and that the eutectic composition lies between Mg_2SiO_4 and $MgSiO_3$. The upper bound reported by Sweeney and Heinz (*3*) or even the higher temperature extrapolation of the data of Zerr and Boehler (*2*) for pure $MgSiO_3$ (Pv) melting are consistent with this suggestion.

Our results imply that the lower mantle of the Earth can be modeled as an intimate mixture of Per + Pv; its solidus temperature is no higher than ~4300 K at ~130 GPa. This temperature would allow partial melting in the lowest reaches of mantle, as recently suggested to explain *P*-wave velocities at the base of the mantle (*19*). Also, this temperature agrees with thermal models of the core, obtained independently by Boehler and by Jeanloz and Morris (*20*) on the basis of melting and Grüneisen parameter mea-

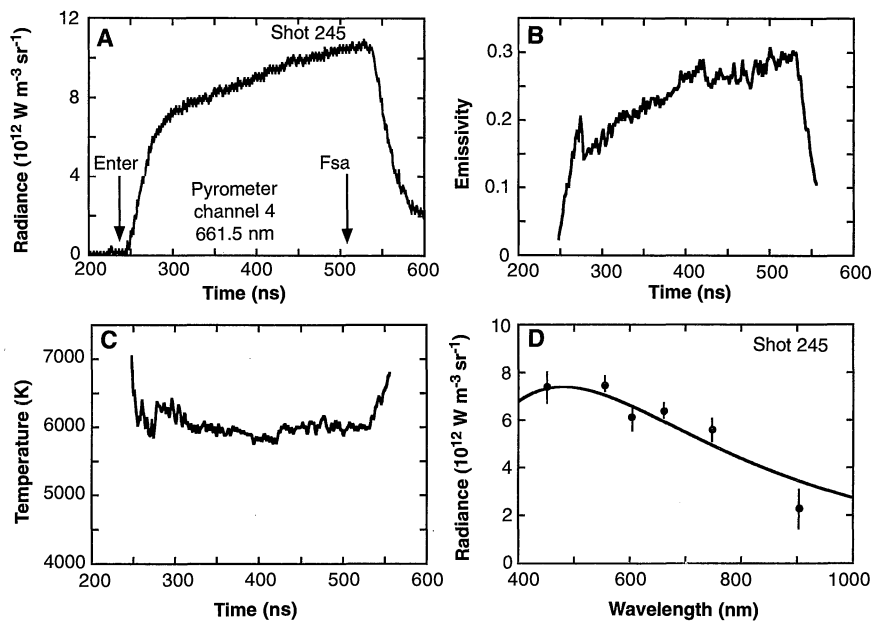

Fig. 2. (**A**) Radiance versus time profile, centered at 650 nm, from shot 245. The time marked "Enter" is the calculated time of arrival of the shock wave at the olivine, and "Fsa" is the calculated time of arrival of the shock wave at the free surface of the olivine. (**B**) Spectral emissivity versus time for shot 245. (**C**) Gray-body temperature versus time for shot 245. (**D**) Spectral fit at 522 ns for shot 245.

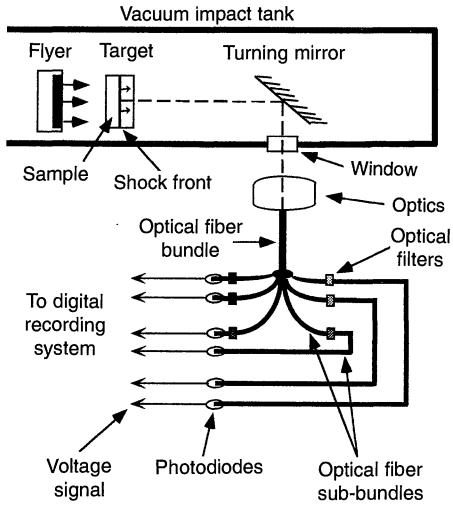

Fig. 1. Schematic diagram of experimental setup (*11*). The flyer is shown in flight before impacting the sample. The shock front is shown as it would appear shortly after impact. The target and the turning mirror are attached to the impact tank, but the flyer is not. The impact tank is evacuated.

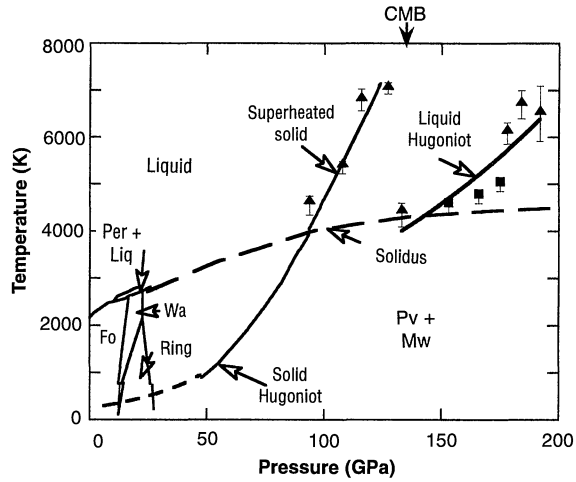

Fig. 3. Pressure-temperature phase diagram for Mg_2SiO_4 and calculated Hugoniot temperature curve for Mg_2SiO_4. When the Hugoniot intersects the solidus, under equilibrium conditions, it follows the solidus until complete melting occurs. However, equilibrium is not achieved, and Hugoniot states achieved overshoot the solidus because of kinetic effects, which results in states along a metastable extension of the solid Hugoniot, a phenomena also observed in SiO_2 (*16*) and KBr and CsBr (*17*). When melting occurs, shock temperatures lie along the solidus, substantially below the temperature of the superheated solid. Experimental shock temperatures are shown intersecting an inferred solidus. Data for San Carlos and Burma peridot are shown as solid triangles, and data for Fo (*8*) are shown as solid squares. Error bars, when not shown, are smaller than symbol size. Mw, magnesiowüstite; Wa, wadsleyite.

Table 1. Temperatures of shocked olivine (hpp). The ΔT and $\Delta\varepsilon$ are root-mean-square uncertainties in temperature and emissivity for ~100 sample times during the last ~100 ns of radiative signal recorded for each shot.

Shot #	Flier-driver material	Pressure (GPa)	Temperature (K)	ΔT (K)	Emissivity	$\Delta\varepsilon$
284	Cu-Cu	93.7	4545	321	0.22	0.15
244	Cu-Cu	107.8	5355	234	0.0132	0.0033
278	Cu-Cu	115.7	6800	201	0.51	0.17
289	Ti-Ti	127.1	7041	315	0.055	0.014
275	Cu-Cu	133.0	4292	270	0.038	0.048
245	Ta-Ta	178.4	6092	310	0.226	0.057
302	Ta-Ta	183.5	6700	213	0.0284	0.0091
303	Ta-Ta	192.0	6510	151	0.298	0.026

surements of outer core candidate components and of downward extrapolation of mantle phase-transition temperatures.

REFERENCES AND NOTES

1. C. J. Allègre *et al.*, *Earth Planet. Sci. Lett.* **134**, 515 (1995); D. J. Weidner, in *Chemistry and Physics of Terrestrial Planets*, S. K. Saxena, Ed. (Springer-Verlag, New York, 1986), pp. 251–274; I. Jackson, *Earth Planet. Sci. Lett.* **62**, 91 (1983); A. E. Ringwood, *Geochim. Cosmochim. Acta* **55**, 2083 (1991).
2. A. Zerr and R. Boehler, *Science* **262**, 553 (1993). The $MgSiO_3$ melting data were measured up to 60 GPa and extrapolated to the pressure of the CMB.
3. E. Knittle and R. Jeanloz, *Geophys. Res. Lett.* **16**, 421 (1989); J. S. Sweeney and D. L. Heinz, in *Proceedings of U.S.–Japan Seminar '96, High Pressure–Temperature Research: Properties of Earth and Planetary Materials*, M. Manghnani and Y. Syono, Eds. (American Geophysical Union, Washington, DC, in press); D. L. Heinz, E. Knittle, J. S. Sweeney, Q. Williams, R. Jeanloz, *Science* **264**, 279 (1994).
4. A. Zerr and R. Boehler, *Nature* **371**, 506 (1994). The data were measured up to 30 GPa and extrapolated to the pressure of the CMB.
5. D. C. Presnall, in (*21*), pp. 248–268.
6. Y. Syono, T. Goto, H. Takei, M. Tokonami, and K. Nobugai [*Science* **214**, 177 (1981)] found that upon shock loading to 78 to 92 GPa, similar-sized samples of Fo disproportionated to MgO (in regions several nanometers in diameter) plus a glass depleted in Si (relative to Mg_2SiO_3). This result is interpreted as demonstrating the occurrence of shock-induced disproportionation of Mg_2SiO_4 to MgO (Per) + $MgSiO_3$ (Pv), where the $MgSiO_3$-rich glass (also in regions several nanometers in diameter) is a high-temperature reversion product of Pv. The diffusion constant inferred for a several-nanometer region of MgO being produced in 10^{-7} s is $\sim 10^{-12.7}$ m^2 s^{-1}. This value is compatible with diffusion data compiled by J. B. Brady [in (*21*), pp. 269–290] for ^{30}Si in olivine (between 1430 and 1830 K).
7. J. M. Brown, M. D. Furnish, D. A. Boness, in *Shock Waves in Condensed Matter-1987*, S. C. Schmidt and N. C. Holmes, Eds. (Elsevier, New York, 1988), pp. 119–122; J. M. Brown, M. D. Furnish, R. G. McQueen, in *High-Pressure Research in Mineral Physics*, M. H. Manghnani and Y. Syono, Eds. (American Geophysical Union, Washington, DC, 1987), pp. 373–384.
8. G. A. Lyzenga, and T. J. Ahrens, *Geophys. Res. Lett.* **7**, 141 (1980).
9. W. Yang, thesis, California Institute of Technology (1996), chap. 4. The new pyrometer has 0.2-mm-diameter photodetectors, which give greater sensitivity and time resolution than our previous detectors but are harder to align. They have a minimum resolvable intensity limit of 0.005 μW cm^{-2} nm^{-1} and a 1-ns rise time, as opposed to 0.25 μW cm^{-2} nm^{-1} and 15 ns, respectively, for the previous pyrometer (*22*).
10. Electron microprobe (JEOL Super Probe) analyses revealed the San Carlos peridot as $(Mg_{0.907},Fe_{0.093})_2SiO_4$ and the Burma peridot as $(Mg_{0.890},Fe_{0.110})_2SiO_4$. Hence, we simply quote the composition of both as $(Mg_{0.9},Fe_{0.1})_2SiO_4$.
11. R. Jeanloz and T. J. Ahrens, in *High-Pressure Research: Applications in Geophysics*, M. H. Manhnani and S. Akimoto, Eds. (Academic Press, San Diego, 1977), pp. 439–461; T. J. Ahrens, *Methods Exp. Phys.* **24**, 185 (1987). In our experiments, a 25-mm-diameter lexan projectile bearing a 1.5-mm-thick Cu, Ti, or Ta flyer plate was accelerated to 5 to 7 km s^{-1} and impacted 0.5-mm-thick Cu, Ti, or Ta driver plates. The planar shock wave induced in the driver plate then propagated into the peridot samples.
12. The sample surface in contact with the driver plate is sputter-coated with an opaque layer of Ag to block light that may originate from the shock-heated driver-sample interface [G. Lyzenga, thesis, California Institute of Technology (1982)].
13. Although the sample emits Planck radiation for ~300 ns, radiative losses do not decrease sample temperature [R. Svendsen and T. J. Ahrens, *Phys. Rep.* **180**, 333 (1989)].
14. Corrections for light absorption upon propagation of light through the unshocked sample was conducted as specified [(*22*); M. B. Boslough, *J. Appl. Phys.* **58** 3394 (1985)]. The ambient transmittance of the sample was measured (*15*) and used to make this correction.
15. The sample transmission spectrum was applied in two different ways in the analysis. It was used to determine the photon fraction absorbed upon propagation from the emitting shock front through the unshocked sample. Transmittance spectra were also used to estimate the wavelength dependence of emissivity ε from the shocked material by Kirchhoff's law. Temperature T and ε are obtained from irradiance I versus wavelength λ by fitting these to

$$I(\lambda) = \frac{\varepsilon C_1 A_s(1 - R_s)(1 - A_u(1 - R_f)}{\lambda^5}(e^{C_2/\lambda T} - 1)^{-1} \quad (1)$$

where $C_1 = 1.19088 \times 10^{-16}$ W·m^2, $C_2 = 1.4388 \times 10^{-2}$ m·K, R_s is the reflectivity of the shocked material–unshocked material interface, R_f is the reflectivity of the unshocked material–vacuum interface at the free surface, and A_s and A_u are the transmission coefficients for the shocked and unshocked materials, respectively. Although ambient-pressure values of transmittance were used to yield a wavelength-dependent emissivity for shocked olivine, this can only be considered an approximation. Both olivine and magnesiowüstite demonstrate marked reddening with increasing pressure at room temperature [M. K. Mao and P. M. Bell, *Science* **176**, 403 (1972); H. K. Mao, *Carnegie Inst. Washington Yearb.* **72**, 554 (1973)].
16. G. A. Lyzenga, T. J. Ahrens, and A. C. Mitchell [*J. Geophys. Res.* **88**, 2431 (1983)] reported similar data for fused and crystal quartz shocked into the stishovite regime that indicated melting of stishovite at 4500 and 4900 K at 70 and 110 GPa, respectively. Recently, static diamond anvil data to 40 GPa were reported in melting data for SiO_2 (stishovite) [G. Y. Shen and P. Lazor, *J. Geophys. Res.* **100**, 17699 (1995)]. These extrapolate closely to the melting line of stishovite inferred by Lyzenga *et al.*; for example, T. J. Ahrens [in *Shock Compression of Condensed Matter*, S. C. Schmidt and W. C. Tao, Eds. (American Institute of Physics, New York, 1996), pp. 3–8] and R. Boehler (private communication) found good agreement between diamond cell and shock-wave data for the melting of NaCl in the B2 structure at 3100 K and 55 GPa. See T. J. Ahrens, G. Lyzenga, A. C. Mitchell, in *High Pressure Research in Geophysics*, S. Akimoto and M. H. Manghnani, Eds. (Center for Academic Publication, Tokyo, 1982), pp. 579–594; see also R. Boehler, in *Advanced Materials '96*, M. Akaishi, Ed. (National Institute for Research in Inorganic Materials, Tsukuba, Japan, 1996), pp. 159–162.
17. D. A. Boness and J. M. Brown [*Phys. Rev. Lett.* **71**, 2931 (1993)] reported shock-temperature and sound-velocity data for KBr and CsBr. They demonstrated that these compounds are superheated and melt at higher pressures. Their behavior is qualitatively similar to that of $(Mg_{0.9},Fe_{0.1})_2SiO_4$ observed here. The data for KBr and CsBr indicate that the temperatures of the melt remain above the solidus. In the case of the Mg_2SiO_4 experiments, we favor the hypothesis that the drop in shock temperature at 130 ± 3 GPa also results from melting; one can also examine whether the temperature decrease could possibly result from a solid-solid phase change. A change in the slope of the pressure-density Hugoniot, which is attributed to melting, is observed at ~140 GPa (*7*). Even if the Brown *et al.* and the present interpretations of the shock temperature data are incorrect, an increase in density for a hypothetical solid-solid phase change (rather than melting) cannot be greater than ~1 to 2%. If the decrease in shock temperature of $\Delta T = 2749°C$ at ~130 GPa were instead associated with a solid-solid reaction, an estimate of the enthalpy change would be given by $\Delta H = C_v\Delta T = 480$ kJ mol^{-1} for a specific heat of $C_v = 3R$ (R is the gas constant, and we assume seven-atom molecules, as in Mg_2SiO_4). This value is considerably greater than the enthalpies associated with melting under equilibrium conditions (~115 kJ mol^{-1}) or the 97 kJ mol^{-1} required for the reaction Mg_2SiO_4 (ringwoodite) → $MgSiO_3$ (Pv) + MgO (Per) at standard temperature and pressure. The lack of a sharp increase in density along the Hugoniot in the Pv and Per regimes taken with the associated drop in sound velocity at ~140 GPa supports the inference that MgO (Per) + $MgSiO_3$ (Pv) is melting from a superheated state and the temperature drop is not easily explained by the onset of polymorphism in olivine.
18. D. C. Presnall and M. J. Walter, *J. Geophys. Res.* **98**, 1977 (1993).
19. E. Garnero and D. V. Helmberger, *Phys. Earth Planet. Inter.* **91**, 161 (1995); E. J. Garnero, S. P. Grand, D. V. Helmberger, *Geophys. Res. Lett.* **20**, 1843 (1993); Q. Williams and E. J. Garnero, *Science* **273**, 1528 (1996). The ultralow-velocity zone is 40 km thick and is marked by a 10% decrease in *P*-wave velocity that is explained by (i) a 30% partial melt if spherical or tubule melting geometry is assumed or (ii) a 5% partial melt if a grain-wetting model is assumed.
20. R. Jeanloz and S. Morris, *Annu. Rev. Earth Planet. Sci.* **14**, 377 (1986); R. Boehler, *ibid.* **24**, 15 (1996).
21. T. J. Ahrens, Ed., *Mineral Physics and Crystallography*, vol. 2 of *A Handbook of Physical Constants* (American Geophysical Union, Washington, DC, 1995).
22. M. B. Boslough and T. J. Ahrens, *Rev. Sci. Instrum.* **60**, 3711 (1988).

23. Research supported by NSF. Division of Geological and Planetary Science, California Institute of Technology, contribution 5672. We thank A. Scherer for the use of his sputtering apparatus, and G. Rossman for the use for of his optical transmission apparatus. We thank P. Wyllie, E. Ohtani, D. Stevenson, M. Gurnis, D. Helmberger, and the reviewers for comments. We also thank E. Gelle, M. Long, and A. Devora for their help in conducting the laboratory experiments.

20 May 1996; accepted 24 January 1997